# Phase Transitions in Even-Even Palladium Isotopes

Sohair M. Diab

*Faculty of Education, Phys. Dept., Ain Shams University, Cairo, Egypt*

E-mail: mppe2@yahoo.co.uk

The positive and negative parity states of the even-even palladium isotopes were studied within the frame work of the interacting boson approximation model (IBA-1). The energy spectra, potential energy surfaces, electromagnetic transition probabilities, back bending and staggering effect have been calculated. The potential energy surfaces show smooth transition from vibrational-like to gamma-soft and finally to rotational-like nuclei. Staggering effectle, has been observed between the positive and negative parity states in palladium isotopes. The agreement between theoretical predictions and experimental values are fairly good.

## 1 Introduction

The region of neutron-excess nuclei at mass $A \cong 100$ is an area of interest to many authors because of the observation of the phase transitions. Three phase transitional regions are well known where the structure changes rapidly. Nd-Sm-Gd and Ru-Pd regions where the change is from spherical to well deformed nuclei when moving from lighter to heavier isotopes. But, Os-Pt regions the change is from well deformed to $\gamma$-soft when moving from lighter to heavier isotopes.

The structure of these transitional nuclei has been the subject of many experimental and theoretical studies. Experimentally, levels of $^{102}$Pd were populated from the decay of $^{102}$Ag populated in the $^{89}$Y ($^{16}$O,3n) reaction [1] and their properties were studied through $\gamma$ spectroscopy. Also, measurements were performed using an array of eight HPGe detectors on gamma multiplicity gated on proton spectra of $^{102\text{-}104}$Pd which have been measured [2] in the $^{12}$C + $^{93}$Np reaction E($^{12}$C) = 40 MeV, at backward angles.The cross-section along with the angular momentum and excitation energy are populated.

Theoretically, the transitional regions and phase transitions in palladium isotopes have been analyzed in the frame work of the IBA-2 model [3–7]. From the analysis of energies, static moments, transition rates, quadrupole moments and mixing ratios, they were able to identify states having large mixed - symmetry components.

Cranked Strutinsky Method [8], Geometric Collective Model [9] (GCM) and the Relativistic Mean Field Theory [10] have examined palladium series of isotopes to find examples displaying the characteristics of E(5) critical point behavior [11]for the shape transition from spherical vibrator to a triaxially soft rotor.

In this article, we carried out a microscopic study of the Yrast and negative parity states, electromagnetic transition rates, $B(E1)$, $B(E2)$, potential energy surfaces, $V(\beta,\gamma)$, for $^{100\text{-}116}$Pd nuclei employing the interacting boson model.

## 2 Interacting boson approximation model (IBA-1)

### 2.1 Level energies

IBA-1 model [12–14 ] was applied to the positive and negative parity states in even-even $^{100\text{-}116}$Pd isotopes. The Hamiltonian employed [15] in the present calculation is:

$$\begin{aligned} H &= EPS \cdot n_d + PAIR \cdot (P \cdot P) \\ &+ \frac{1}{2} ELL \cdot (L \cdot L) + \frac{1}{2} QQ \cdot (Q \cdot Q) \\ &+ 5OCT \cdot (T_3 \cdot T_3) + 5HEX \cdot (T_4 \cdot T_4), \end{aligned} \tag{1}$$

where

$$P \cdot p = \frac{1}{2} \left[ \begin{array}{l} \left\{ (s^\dagger s^\dagger)_0^{(0)} - \sqrt{5} (d^\dagger d^\dagger)_0^{(0)} \right\} x \\ \left\{ (ss)_0^{(0)} - \sqrt{5} (\tilde{d}\tilde{d})_0^{(0)} \right\} \end{array} \right]_0^{(0)}, \tag{2}$$

$$L \cdot L = -10\sqrt{3} \left[ (d^\dagger \tilde{d})^{(1)} x \, (d^\dagger \tilde{d})^{(1)} \right]_0^{(0)}, \tag{3}$$

$$Q \cdot Q = \sqrt{5} \left[ \begin{array}{l} \left\{ (S^\dagger \tilde{d} + d^\dagger s)^{(2)} - \frac{\sqrt{7}}{2} (d^\dagger \tilde{d})^{(2)} \right\} x \\ \left\{ (s^\dagger \tilde{d} + + \tilde{d}s)^{(2)} - \frac{\sqrt{7}}{2} (d^\dagger \tilde{d})^{(2)} \right\} \end{array} \right]_0^{(0)}, \tag{4}$$

$$T_3 \cdot T_3 = -\sqrt{7} \left[ (d^\dagger \tilde{d})^{(2)} x \, (d^\dagger \tilde{d})^{(2)} \right]_0^{(0)}, \tag{5}$$

$$T_4 \cdot T_4 = 3 \left[ (d^\dagger \tilde{d})^{(4)} x \, (d^\dagger \tilde{d})^{(4)} \right]_0^{(0)}. \tag{6}$$

In the previous formulas, $n_d$ is the number of boson; $P \cdot P$, $L \cdot L$, $Q \cdot Q$, $T_3 \cdot T_3$ and $T_4 \cdot T_4$ represent pairing, angular momentum, quadrupole, octupole and hexadecupole interactions between the bosons; $EPS$ is the boson energy; and $PAIR$, $ELL$, $QQ$, $OCT$, $HEX$ is the strengths of the pairing, angular momentum, quadrupole, octupole and hexadecupole interactions.

| nucleus | $EPS$ | $PAIR$ | $ELL$ | $QQ$ | $OCT$ | $HEX$ | $E2SD(eb)$ | $E2DD(eb)$ |
|---|---|---|---|---|---|---|---|---|
| $^{100}$Pd | 0.6780 | 0.000 | 0.0095 | −0.020 | 0.0000 | 0.0000 | 0.1020 | −0.3817 |
| $^{102}$Pd | 0.5840 | 0.000 | 0.0115 | −0.0200 | 0.0000 | 0.0000 | 0.1270 | −0.3757 |
| $^{104}$Pd | 0.5750 | 0.0000 | 0.0225 | −0.0200 | 0.0000 | 0.0000 | 0.1210 | −0.3579 |
| $^{106}$Pd | 0.5630 | 0.0000 | 0.0230 | −0.0200 | 0.0000 | 0.0000 | 0.1220 | −0.3609 |
| $^{108}$Pd | 0.5180 | 0.0000 | 0.0235 | −0.0200 | 0.0000 | 0.0000 | 0.1170 | −0.3461 |
| $^{110}$Pd | 0.4950 | 0.0000 | 0.0235 | −0.0200 | 0.0000 | 0.0000 | 0.1110 | −0.3283 |
| $^{112}$Pd | 0.4950 | 0.0000 | 0.0235 | −0.0200 | 0.0000 | 0.0000 | 0.08770 | −0.2594 |
| $^{114}$Pd | 0.52200 | 0.0000 | 0.0235 | −0.0200 | 0.0000 | 0.0000 | 0.0612 | −0.1810 |
| $^{116}$Pd | 0.5700 | 0.0000 | 0.0216 | −0.0200 | 0.0000 | 0.0000 | 0.0742 | −0.2195 |

Table 1: Parameters used in IBA-1 Hamiltonian (all in MeV).

### 2.2 Electromagnetic transition rates

The electric quadrupole transition operator [15] employed in this study is:

$$T^{(E2)} = E2SD \cdot (s^{\dagger}\tilde{d} + d^{\dagger}s)^{(2)} + \\ + \frac{1}{\sqrt{5}} E2DD \cdot (d^{\dagger}\tilde{d})^{(2)} . \qquad (7)$$

The reduced electric quadrupole transition rates between $I_i \to I_f$ states are given by

$$B(E_2, I_i - I_f) = \frac{[< I_f \parallel T^{(E_2)} \parallel I_i >]^2}{2I_i + 1} . \qquad (8)$$

## 3 Results and discussion

### 3.1 The potential energy surfaces

The potential energy surfaces [16], $V(\beta, \gamma)$, as a function of the deformation parameters $\beta$ and $\gamma$ are calculated using:

$$\begin{aligned} &E_{N_{\Pi} N_{\nu}}(\beta,\gamma) = <N_{\pi}N_{\nu};\beta\gamma\,|H_{\pi\nu}|N_{\pi}N_{\nu};\beta\gamma> \\ &= \zeta_d(N_{\nu}N_{\pi})\beta^2(1+\beta^2) + \beta^2(1+\beta^2)^{-2}\times \\ &\times \left\{kN_{\nu}N_{\pi}[4 - (\bar{X}_{\pi}\bar{X}_{\nu})\beta\cos 3\gamma]\right\} + \\ &+ \left\{[\bar{X}_{\pi}\bar{X}_{\nu}\beta^2] + N_{\nu}(N_{\nu}-1)\left(\frac{1}{10}c_0 + \frac{1}{7}c_2\right)\beta^2\right\} , \end{aligned} \qquad (9)$$

where

$$\bar{X}_{\rho} = \left(\frac{2}{7}\right)^{0.5} X_{\rho} \quad \rho = \pi \text{ or } \upsilon . \qquad (10)$$

The calculated potential energy surfaces, $V(\beta, \gamma)$, are presented in Fig. 1. It shows that $^{100-110}$Pd are vibrational-like nuclei while $^{112}$Pd is a $\gamma$-soft where the two wells on the oblate and prolate sides are equal. $^{114,116}$Pd are prolate deformed and have rotational characters. So, $^{112}$Pd is thought to be a transitional nucleus forming a zone between soft vibration side and nearly deformed nuclei in the other side.

### 3.2 Energy spectra

The energy of the positive and negative parity states of palladium series of isotopes are calculated using computer code PHINT [17]. A comparison between the experimental spectra [18–26] and our calculations for the ground state and $(-ve)$ parity states are illustrated in Fig. 2. The model parameters given in Table 1 are free parameters and adjusted to reproduce as closely as possible the excitation energy of the $(+ve)$ and $(-ve)$ parity levels. The agreement between the calculated levels energy and their correspondence experimental values for all nuclei are slightly higher for the higher excited states. We believe this is due to the change of the projection of the angular momentum which is due mainly to band crossing.

Unfortunately there is no enough measurements of electromagnetic transition rates $B(E1)$ or $B(E2)$ for these series of nuclei. The only measured $B(E2, 0_1^+ \to 2_1^+)$'s are presented, in Table 2 for comparison with the calculated values. The parameters $E2SD$ and $E2DD$ are displayed in Table 1 and used in the computer code NPBEM [17] for calculating the electromagnetic transition rates after normalization to the available experimental values.

No new parameters are introduced for calculating electromagnetic transition rates $B(E2)$, (Table 1), and $B(E1)$, (Table 2), of intraband and interband. The values of the ground state band are presented in Fig. 3 and show bending at $N = 64$ which means there is an interaction between the $(+ve)$ ground state and the $(-ve)$ parity states.

The moment of inertia $I$ and angular frequency $\hbar\omega$ are calculated using equations (11, 12):

$$\frac{2J}{\hbar^2} = \frac{4I - 2}{\Delta E(I \to I - 2)} , \qquad (11)$$

$$(\hbar\omega)^2 = (I^2 - I + 1)\left[\frac{\Delta E(I \to I - 2)}{(2I - 1)}\right]^2 . \qquad (12)$$

The plots in Fig. 4 show upper bending at $I^+ = 12$ and lower bending at $I^+ = 14$ for $^{100\text{-}116}$Pd. It means, there is a crossing between the ground and the $(-ve)$ parity states.

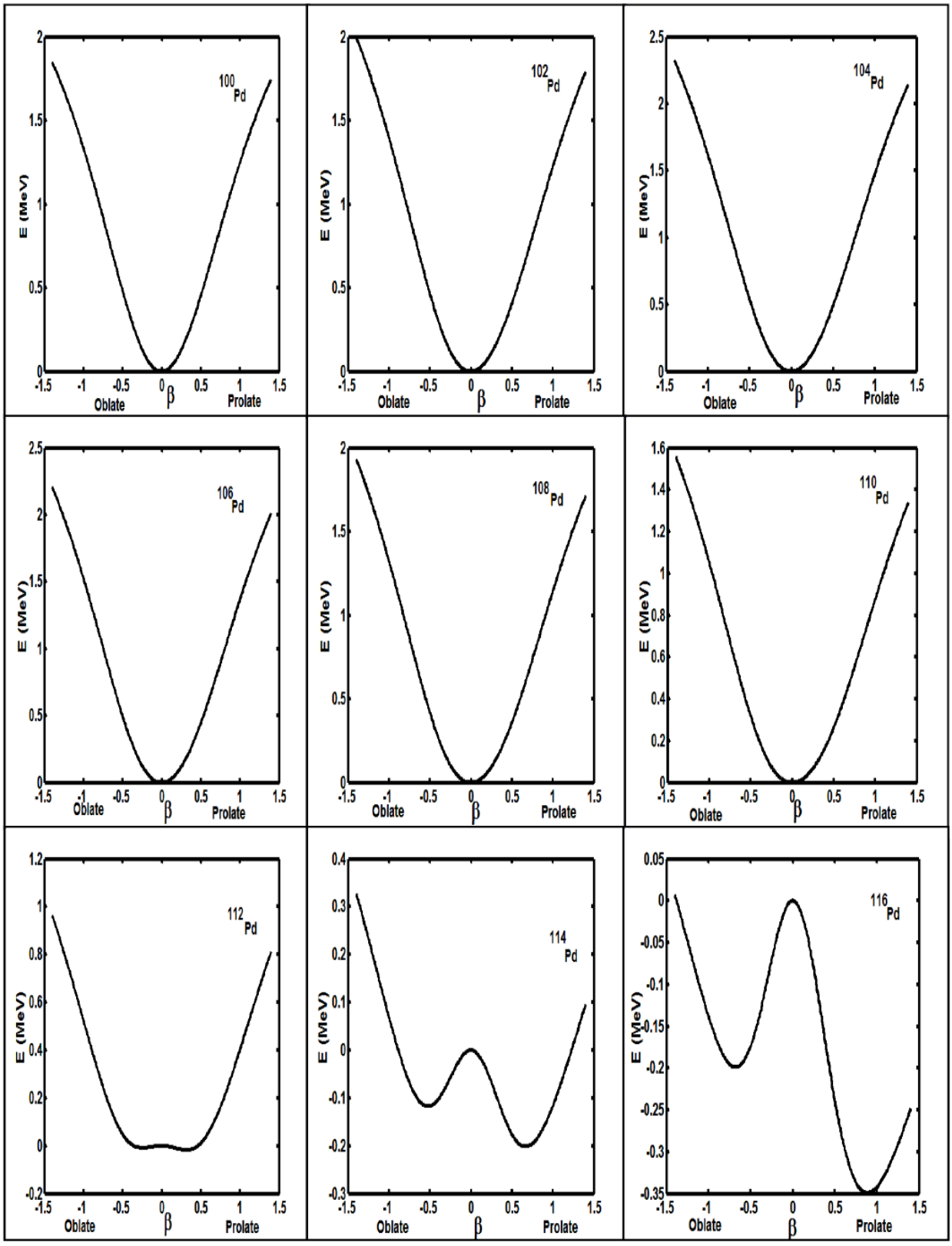


Fig. 1: Potential energy surfaces for $^{100\text{-}116}$Pd nuclei.

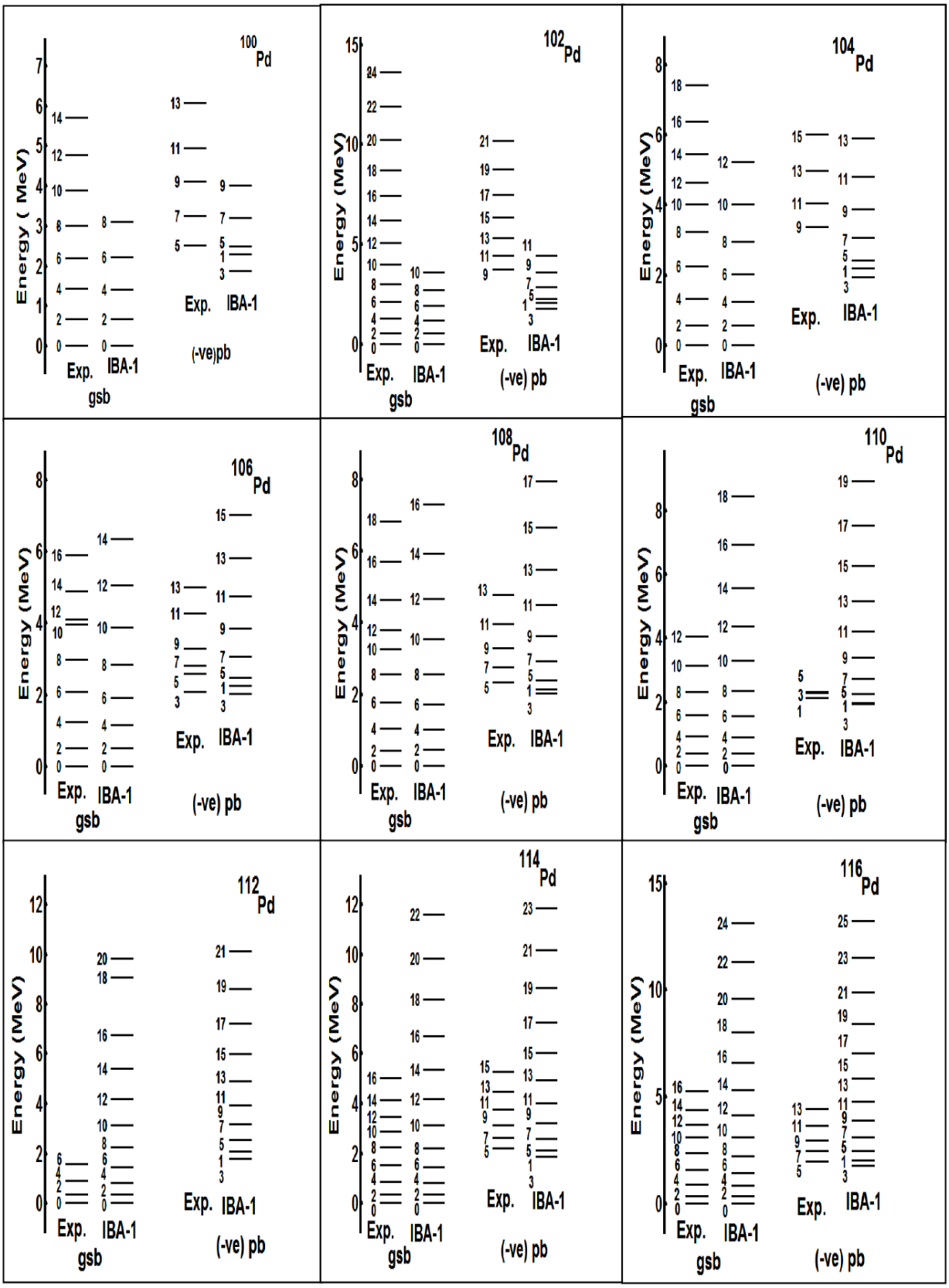


Fig. 2: Comparison between exp. [18–26] and theoretical (IBA-1) energy levels.

| $I_i^+$ $I_f^+$ | $^{100}$Pd | $^{102}$Pd | $^{104}$Pd | $^{106}$Pd | $^{108}$Pd | $^{110}$Pd | $^{112}$Pd | $^{114}$Pd | $^{116}$Pd |
|---|---|---|---|---|---|---|---|---|---|
| $0_1$ Exp*. $2_1$ | —— | 0.460(30) | 0.535(35) | 0.660(35) | 0.760(40) | 0.870(40) | 0.660(11) | 0.380(20) | 0.620(18) |
| $0_1$ Theor. $2_1$ | 0.2275 | 0.4657 | 0.5317 | 0.6663 | 0.7672 | 0.8631 | 0.6640 | 0.3804 | 0.6237 |
| $2_1$ $0_1$ | 0.0455 | 0.0931 | 0.1063 | 0.13333 | 0.1534 | 0.1726 | 0.1328 | 0.0761 | 0.1247 |
| $2_2$ $0_1$ | 0.0001 | 0.0004 | 0.0007 | 0.0013 | 0.0023 | 0.0034 | 0.0029 | 0.0017 | 0.0028 |
| $2_2$ $0_2$ | 0.0199 | 0.0395 | 0.0449 | 0.0582 | 0.0738 | 0.0925 | 0.0785 | 0.0481 | 0.0819 |
| $2_3$ $0_1$ | 0.0000 | 0.0000 | 0.0000 | 0.0000 | 0.0001 | 0.0004 | 0.0007 | 0.0006 | 0.0010 |
| $2_3$ $0_2$ | 0.0286 | 0.0669 | 0.0822 | 0.1051 | 0.1126 | 0.1100 | 0.0704 | 0.0356 | 0.0576 |
| $2_3$ $0_3$ | 0.0045 | 0.0082 | 0.0095 | 0.0128 | 0.0180 | 0.0270 | 0.0260 | 0.0166 | 0.0292 |
| $2_4$ $0_3$ | 0.0012 | 0.0044 | 0.0074 | 0.0129 | 0.0234 | 0.0423 | 0.0462 | 0.0317 | 0.0570 |
| $2_4$ $0_4$ | 0.0335 | 0.0602 | 0.0640 | 0.0755 | 0.0744 | 0.0702 | 0.0398 | 0.0182 | 0.0279 |
| $4_1$ $2_1$ | 0.0702 | 0.1545 | 0.1846 | 0.2396 | 0.2943 | 0.3265 | 0.2535 | 0.1463 | 0.2429 |
| $4_1$ $2_2$ | 0.0071 | 0.0137 | 0.0156 | 0.0202 | 0.0249 | 0.0300 | 0.0245 | 0.0150 | 0.0264 |
| $4_1$ $2_3$ | 0.0117 | 0.0278 | 0.0346 | 0.0449 | 0.0492 | 0.0492 | 0.0323 | 0.0168 | 0.0277 |
| $6_1$ $4_1$ | 0.0711 | 0.1756 | 0.2236 | 0.3011 | 0.3635 | 0.4188 | 0.3244 | 0.1878 | 0.3153 |
| $6_1$ $4_2$ | 0.0098 | 0.0177 | 0.0195 | 0.0241 | 0.0273 | 0.0304 | 0.0233 | 0.0139 | 0.0244 |
| $6_1$ $4_3$ | 0.0062 | 0.0191 | 0.0261 | 0.0353 | 0.0384 | 0.0380 | 0.0250 | 0.0131 | 0.0218 |
| $8_1$ $6_1$ | 0.0476 | 0.1559 | 0.2225 | 0.3180 | 0.3950 | 0.4613 | 0.3599 | 0.2102 | 0.3574 |
| $8_1$ $6_2$ | 0.0107 | 0.0184 | 0.0197 | 0.0236 | 0.0252 | 0.0266 | 0.0198 | 0.0116 | 0.0205 |
| $8_1$ $6_3$ | —— | 0.0094 | 0.0169 | 0.0253 | 0.0288 | 0.0295 | 0.0201 | 0.0109 | 0.0185 |
| $10_1$ $8_1$ | —— | 0.0969 | 0.1835 | 0.2936 | 0.3849 | 0.4629 | 0.3679 | 0.2183 | 0.3769 |
| $10_1$ $8_2$ | —— | 0.0178 | 0.0187 | 0.0219 | 0.0224 | 0.0229 | 0.0166 | 0.0096 | 0.0171 |

Table 2: Values of the theoretical reduced transition probability, $B(E2)$ (in $e^2\,b^2$).
*Ref. 27.

| $I_i^-$ $I_f^+$ | $^{100}$Pd | $^{102}$Pd | $^{104}$Pd | $^{106}$Pd | $^{108}$Pd | $^{110}$Pd | $^{112}$Pd | $^{114}$Pd | $^{116}$Pd |
|---|---|---|---|---|---|---|---|---|---|
| $1_1$ $0_1$ | 0.0009 | 0.0020 | 0.0033 | 0.0052 | 0.0091 | 0.0148 | 0.0213 | 0.0255 | 0.0259 |
| $1_1$ $0_2$ | 0.1290 | 0.1248 | 0.1299 | 0.1314 | 0.1340 | 0.1360 | 0.1369 | 0.1379 | 0.1384 |
| $3_1$ $2_1$ | 0.1268 | 0.1228 | 0.1235 | 0.1246 | 0.1309 | 0.1414 | 0.1530 | 0.1605 | 0.1617 |
| $3_1$ $2_2$ | 0.0267 | 0.0361 | 0.0395 | 0.0443 | 0.0501 | 0.0566 | 0.0645 | 0.0719 | 0.0771 |
| $3_1$ $2_3$ | 0.0006 | 0.0018 | 0.0030 | 0.0053 | 0.0108 | 0.0190 | 0.0268 | 0.0311 | 0.0335 |
| $3_2$ $2_1$ | 0.0093 | 0.0031 | 0.0016 | 0.0012 | 0.0014 | 0.0028 | 0.0053 | 0.0079 | 0.0099 |
| $3_2$ $2_2$ | 0.0912 | 0.0278 | 0.0190 | 0.0153 | 0.0136 | 0.0146 | 0.0172 | 0.0196 | 0.0193 |
| $3_2$ $2_3$ | 0.1132 | 0.2103 | 0.2247 | 0.2243 | 0.2172 | 0.2109 | 0.1827 | 0.1686 | 0.1599 |
| $5_1$ $4_1$ | 0.2660 | 0.2582 | 0.2578 | 0.2576 | 0.2637 | 0.2747 | 0.2873 | 0.2959 | 0.2979 |
| $5_1$ $4_2$ | 0.0260 | 0.0392 | 0.0457 | 0.0530 | 0.0604 | 0.0670 | 0.0736 | 0.0801 | 0.0861 |
| $5_1$ $4_3$ | 0.0002 | 0.0010 | 0.0018 | 0.0032 | 0.0058 | 0.0088 | 0.0111 | 0.0125 | 0.0137 |
| $7_1$ $6_1$ | 0.415* | 0.4035 | 0.4005 | 0.3982 | 0.4025 | 0.4121 | 0.4236 | 0.4319 | 0.4341 |
| $7_1$ $6_2$ | 0.0163 | 0.0325 | 0.0419 | 0.0515 | 0.0598 | 0.0663 | 0.0722 | 0.0781 | 0.0844 |
| $9_1$ $8_1$ | 0.5714 | 0.5561 | 0.5489 | 0.5439 | 0.5454 | 0.5524 | 0.5617 | 0.5689 | 0.5709 |
| $9_1$ $8_2$ | —— | 0.0187 | 0.0318 | 0.0436 | 0.0533 | 0.0604 | 0.0664 | 0.0725 | 0.0792 |
| $11_1$ $10_1$ | —— | 0.7143 | 0.7015 | 0.6933 | 0.6914 | 0.6950 | 0.7017 | 0.7073 | 0.7088 |

Table 3: Values of the theoretical reduced transition probability, $B(E1)$ (in $\mu\,e^2b$).

This fact has confirmed by studying the staggering effect to palladium isotopes which presented in Fig.5.

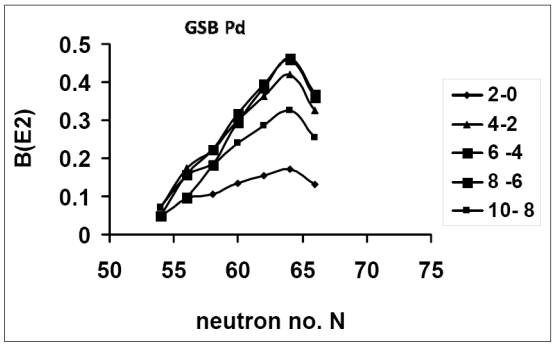


Fig. 3: The calculated $B(E2)$'s for the ground state band.

### 3.3 The staggering

The presence of $(+ve)$ and $(-ve)$ parity states has encouraged us to study staggering effect [28–30] for $^{100\text{-}116}$Pd series of isotopes using staggering function equations (15, 16) with the help of the available experimental data [18–26].

$$Stag(I) = 6\Delta E(I) - 4\Delta E(I-1) - 4\Delta E(I+1) + \Delta E(I+2) + \Delta E(I-2), \quad (13)$$

with

$$\Delta E(I) = E(I+1) - E(I). \quad (14)$$

The calculated staggering patterns are illustrated in Fig. 5 which show an interaction between the $(+ve)$ and $(-ve)$ parity states of $^{100\text{-}104}$Pd and $^{112\text{-}1116}$Pd nuclei at $I^+ = 12$. Unfortunatelly, there is no enough experimental data are available for $^{106\text{-}110}$Pd to study the same effect.

### 3.4 Conclusions

IBA-1 model has been applied successfully to $^{100\text{-}116}$Pd isotopes and we have got:

1. The levels energy are successfully reproduced;
2. The potential energy surfaces are calculated and show vibrational-like to $^{100-110}$Pd, $\gamma$-soft to $^{112}$Pd and rotational characters to $^{114\text{-}116}$Pd isotopes where they are mainly prolate deformed nuclei;
3. Electromagnetic transition rates $B(E1)$ and $B(E2)$ are calculated;
4. Upper bending for $^{100\text{-}106}$Pd has been observed at angular momentum $I^+ = 12$ and lower bending at $I^+ = 14$ for all palladium isotopes;
5. Electromagnetic transition rates $B(E1)$ and $B(E2)$ are calculated;and

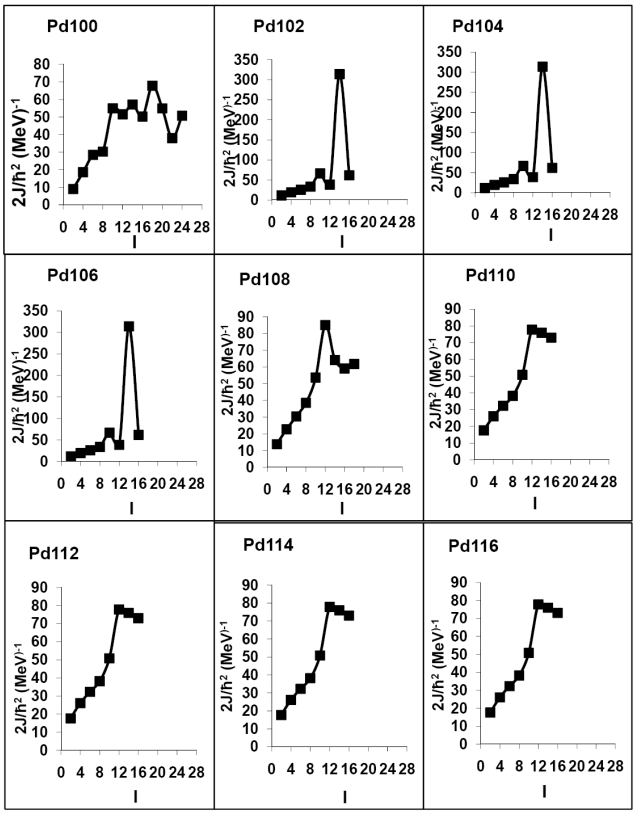


Fig. 4: Angular momentum $I$ as a function of $2J/\hbar^2$.

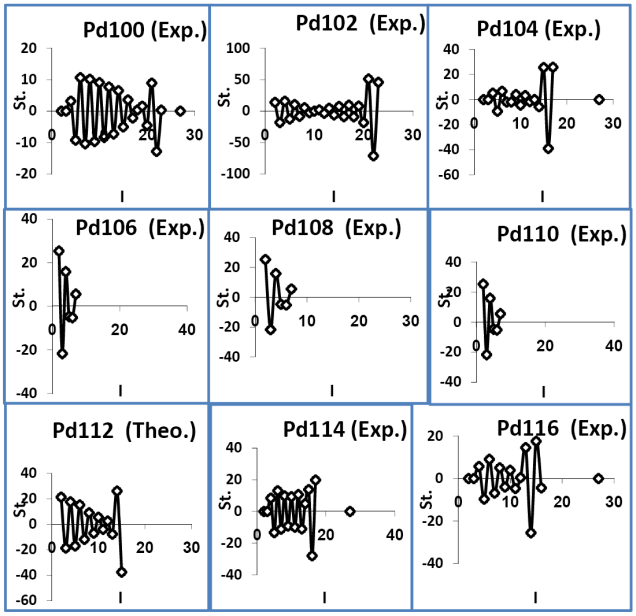


Fig. 5: $\Delta I = 1$, staggering patterns for $^{100\text{-}116}$Pd isotopes.

6. Staggering effect and beat patterns are observed and show an interaction between the $(-\mathtt{ve})$and $(+\mathtt{ve})$ parity states at $I^{+}=12$ for palladium isotopes except for $^{106\text{-}110}$Pd where scarce experimental data are available.

Submitted on September 02, 2008
Accepted on October 17, 2008

## References

1. Zamfir N. V., Capiro M. A., Casten R. F., Barton C. J., Beausang C. W., Berant Z., Bernner D. S., Chou W. T., Cooper J. R., Hecht A. A., Krucken R., Newman H., Novak J. R., Pietralla N., Wolf A. and Zyromski K. E. *Phys. Rev. C*, 2002, v. 65, 044325.
2. Mitra A., Chakrabarty D. R., Datar V. M.,Kumar S., Mirgule E. T., Oza H. H., Nanal V., Pillay R. G. *Nucl. Phys. A*, 2006, v. 765, 277.
3. Bharti A. and Khosa S. K. *Phys. Rev. C*, 1996, v. 53, 2528.
4. Giannatiempo A., Nannini A. and Sona P. *Phys. Rev. C*, 1998, v. 58, 3316.
5. Giannatiempo A., Nannini A. and Sona P. *Phys. Rev. C*, 1998, v. 58, 3335.
6. Pan F. and Draayer J. P. *Nucl. Phys. A*, 1998, v. 636, 156.
7. Garcia-Ramos J. E., De Coster C., Fossion R. and Heyde K. *Nucl. Phys. A*, 2001, v. 688, 735.
8. Chasman R. R. *Phys. Rev. C*, 2001, v. 64, 024311.
9. Caprio M. A. *Phys. Rev. C*, 2003, v. 68, 054303.
10. Fossion R., Bonatsos D. and Lalazissis G. A. *Phys. Rev. C*, 2006, v. 73, 044310.
11. Clark R. M., Cromaz M., Deleplanque M. A., Descovich M., Diamond R. M., Fallon P., Lee I. Y., Macchiavelli A. O., Mahmud H., Rodriguez-Vieitez E., Stephens F.S., and Ward D. *Phys. Rev. C*, 2004, v. 69, 064322.
12. Arima A. and Iachello F. *Ann. Phys. (N.Y.)*, 1976, v. 99, 253.
13. Arima A. and Iachello F. *Ann. Phys. (N.Y.)*, 1978, v. 111, 201.
14. Arima A. and Iachello F. *Ann. Phys. (N.Y.)*, 1979, v. 123, 468.
15. Feshband H. and Iachello F. *Ann. Phys.*, 1974, v. 84, 211.
16. Ginocchio J. N. and Kirson M. W. *Nucl. Phys. A*, 1980, v. 350, 31.
17. Scholten O. *The programm package PHINT (1980) version, internal report KVI-63, Gronigen: Keryfysisch Versneller Institut*.
18. Balraj Singh *Nucl. Data Sheets*, 2008, v. 109, 297.
19. Frenne D. D. and Jacobs E. *Nucl. Data Sheets*, 1998, v. 83, 535.
20. Blachot J. *Nucl. Data Sheets*, 2007, v. 108, 2035.
21. Frenne D. D. and Negret A. *Nucl. Data Sheets*, 2008, v. 109, 943.
22. Blachot J. *Nucl. Data Sheets*, 2000, v. 91, 135.
23. Frenne D. D. and Jacobs E. *Nucl. Data Sheets*, 2000, v. 89, 481.
24. Frenne D. D. and Jacobs E. *Nucl. Data Sheets*, 1996, v. 79, 639.
25. Blachot J. *Nucl. Data Sheets*, 2002, v. 97, 593.
26. Blachot J. *Nucl. Data Sheets*, 2001, v. 92, 455.
27. Raman S., de Nestor C. W. and Tikkanen P. *Atomic Data and Nucl. Data Tab.*, 2001, v. 78, 1.
28. Minkov N., Yotov P., Drenska S. and Scheid W. *J. Phys. G*, 2006, v. 32, 497.
29. Bonatsos D., Daskaloyannis C., Drenska S. B., Karoussos N., Minkov N., Raychev P. P. and Roussev R. P. *Phys. Rev. C*, 2000, v. 62, 024301.
30. Minkov N., Drenska S. B., Raychev P. P., Roussev R. P.and Bonatsos D. *Phys. Rev. C*, 2001, v. 63, 044305.